Total manuscript pages: 28 [1]

Precise Localisation of Archaeological Findings with a new Ultrasonic 3D Positioning Sensor

A.R. Jiménez and F. Seco

Instituto de Automática Industrial - CSIC
Ctra. Campo Real km 0.2 La Poveda
28500 Arganda del Rey. Madrid (Spain)
FAX:34 91 871 70 50
e-mail: arjimenez@iai.csic.es
Web: www.iai.csic.es/lopsi

[1] Published in: Sensors and Actuators A: Physical, Volumes 123-124, 23 September 2005, Pages 224-233. http://dx.doi.org/10.1016/j.sna.2005.03.064

Abstract

This paper presents a new ultrasonic sensor for 3D co-ordinate estimation, which has been especially designed to localize and sketch findings after they are extracted by archaeologists. Classical tasks at paleo-archaeological excavations are: measuring position with metric tapes, drawing a sketch of found object, and introducing all information into a database manually; operations that are not efficient and prone to errors. The positioning system we have designed allows simultaneous characterization of several findings (absolute position, shape, size and orientation) using as a tool a wireless 2-metre-long rod, whose lower tip has to be placed on the object under study. The system contains two ultrasonic emitters and employs the time-of-flight (TOF) the ultrasonic signal takes to reach several fixed receivers, and a robust trilateration algorithm to determine the position of the rod tip with 10 mm accuracy. Object position and contour information are automatically transferred to a database in a central computer avoiding manual typewriting. Airflow is the main source of positioning error in outdoor environments, so a strategy based on a differential emitter fixed at a known position is used, which permits to cancel out the effects of uniform air motion.

Key words: Ultrasound, Trilateration, Localisation, Archaeology, Wind Speed

1 Introduction

The typical way of operation in a paleo-archaeological excavation could be described as consisting in five stages: 1) Precise and slow digging in an archaeological excavation till findings are obtained; 2) Measurement of the three-dimensional position of each finding by manually measuring distances to a reticule used as a reference; 3) Registration in a notebook of other data related to the findings, such as, taxonomy, shape, orientation, drawings, etc.; 4) Manually typing data into an electronic database; and finally, 5) Analysis of the data obtained, especially the spatial relationship among near findings. The first four stages are performed sequentially or even simultaneously during the excavation period (summer season), while the fifth stage is performed afterwards (rest of the year) in a laboratory [1].

The working area is organized with cords creating a mesh of several square cells with 1 meter-long sides. Each cell is assigned with an unique identification code consisting in a letter followed by a number. Three sources of error are associated to this positioning system (see figure 1): (a) systematic errors within a cell caused by bad reticule positioning (up to 10 cm); (b) inaccurate positioning measurement within a cell that is normally done using a metric tape; and (c) cell misidentification, which always leads to errors larger than 1

m. Summarizing, the traditional reticule method is inaccurate and subject to many errors.

There are also some other traditional tasks that are time-consuming and not efficient. For example, archaeological findings greater than 1 centimeter square are manually drawn to preserve a record of their orientation, size and shape. Thus, it is spent a lot of time getting an artistic, but also not too accurate graphical representation of the found object. Additionally, all registered data has to be transferred from the paper (e.g. notebook, agenda,) to an electronic database, by manual typewriting, for future analysis in the laboratory.

From the above-mentioned problems, it is clear the need of a measuring system that automates most of the tasks described in stages 2, 3 and 4 (see first paragraph). This device should provide an efficient and reliable solution for measuring the 3D-coordinate of each finding; it should allow drawing its profile defining its shape, size and orientation; and it should have an interface for exporting the data to the server storing the archeological database.

There are many research solutions developed for position estimation of an object of interest [2,3]. Most of them are based on triangulation and multilateration methods using light [4,5], ultrasound [6–12], or radio signals [13–15], and they are capable of estimating the absolute position co-ordinates. Other techniques, give relative positioning, such as, inertial or odometric methods but accumulate errors with time and need a re-calibration periodically. None of the existing solutions were directly applicable to our objectives.

Therefore, a 3D positioning system based on ultrasonic trilateration was designed for this application. To select this technology we considered requirements like minimum interference with the archaeological setups, easiness of operation, low cost, and extensibility to large excavation sites. One very important drawback of ultrasonic based sensors is the the sensitivity to environmental conditions like temperature fluctuations, air turbulence, transducer occlusion or specular reflections. Compensating techniques to eliminate or attenuate the influence of these factors are implemented in our sensor.

The results of the proposed location sensor fulfil our requirements. The device replaces the reticule with a set of eight ultrasonic receivers, which are enough to cover an area of 4x4 m, and guarantee a positioning precision of 10 mm. The sensor system permits position measurement and object profiling, with minimal interference with the normal procedure of excavation. The user can configure the system through an easy interface, and finally, data corresponding to each finding can be transfered to other external equipment, such as desktop or palm computers, via RS-232 and TCP/IP protocols.

Next sections describe the design of the proposed ultrasound sensor, its way of use, the estimation method using a redundant configuration, the differential

measurement method used to diminish airflow influence, and finally, the results and a discussion.

2 Sensor description

2.1 Design

The design concept and way of operation of the sensor device presented in this paper is explained with the help of fig. 2. There is a network made of eight receivers placed in pairs on vertical rods at fixed positions. The positioning tool is a 2-metre-long wireless portable rod which carries two emitters placed in the middle and top part (their separation is approximately 70 cm). The reason why a rod with two emitters has been chosen is that the line of sight between emitters an receivers must be kept free for ultrasound propagation. So, using this configuration with both emitters above the heads of the majority of archeologist in the excavation, there will be a greater number of valid measurements. The use of two emitters on the rod also allows to infer their inclination in space, and therefore where the lower tip of the rod is pointing at. There is also a third emitter located at a fixed position inside the workspace. This third emitter is placed to diminish the influence of airflow onto the times of flight (TOF) measured, as well as, to check the system integrity, and to eliminate possible systematic errors. More details about its way of operation are described in section 4. As sketched in figure 2, several emitter rods can operate simultaneously, sharing the same receiver frame network. From the point of view of the user, the simultaneous operation of several rods in the same working space is a fact. However, the system performs an ad-hoc TDMA (Time Division Multiple Access) approach avoiding mutual signal interference. This kind of time multiplexing, which is performed at time slots of approximately 100 ms, makes the user to perceive the measuring process as being performed in parallel to other user's measurements.

The use of the portable rod by the archaeologist is easy and intuitive. The archaeologist places the lower extreme of the rod on the object to locate (fig. 2). The rod must be kept approximately upright, but it is not necessary to keep it perfectly vertical. The system has been designed for operation in two modes (selectable from the tool): position measurement and object contour tracing. In the first case the system captures the 3D position of the rod tip whenever the user pushes a button in the rod. In the second the trajectory of the rod tip is continuously acquired by the system, and the worker uses the rod as a stylus, following the contour of the object under study.

The whole system can be divided in two main modules: the portable rod module, and the static control module (Fig. 3). The portable rod is wireless and has its own circuitry powered by a battery. A Liquid Crystal Display (LCD) is used for user feedback presenting alphanumeric information such as current position, battery status, and additional messages or warnings. When a archeologist push the start button on the rod, the circuitry associated to the rod is switched on and a PIC micro-controller sends a request of emission via radio-frequency to the control module. Once the control module granted the permission for emission, both ultrasound transducers at the portable rod are immediately excited with a train of pulses.

The control module performs the signal acquisition of the eight receiving channels and computes the times of flight (TOF). Then, the position of each emitter and the position of the finding are computed using algorithms explained in section 3. The PIC micro-controller embedded in the PC, when receiving a request for emission from a new rod, determines if there is another one using the system and, if the system is free, then gives the control to the requesting rod. During all the process, the synchronization is made using RF signals at 418 and 433 MHz.

Currently, the system supports up to 32 rods operating in parallel by time multiplexing. It means that the control module sets up a schedule for sequential positioning of the rods, preventing overlap of the ultrasonic signals. The wireless communication and synchronization of multiple rods is achieved thanks to a RF series protocol designed especially for this application and implemented on the micro-controllers. This protocol has associated several functions: identification tasks, determination of RF coverage in both directions to determine whether communication is possible or not, synchronization tasks and rod management. If workspace has to be extended to cover larger excavation sites, it can be done by adding extra groups of eight receivers, which also implies additional data acquisition and signal-conditioning cards at the PC.

The system has an open interface for transmission of position information. It sends information such as 3D co-ordinate, mode of operation (positioning or drawing), precision, reliability, and the identification code of the rod under measurement. Currently, the connectivity is supported via TCP/IP and RS-232.

Ultrasonic transducers are used as emitters and receivers. The emitters used in the rods are omni-directional PVDF piezoelectric polymer transducers by MSI [16], with a resonant frequency of 40 kHz (8 kHz Bandwidth) and needing a recommended excitation voltage of 300 V (see figure 4). It is clear from this figure than this cylindrical transducer is omnidirectional in the horizontal plane, however the lobe in the vertical direction has a divergence of ± 40 degrees (at -6 dB). That is the reason why it is not strictly required to keep the mobile rod vertically while measuring. Considering that receivers at fixed posts are separated a little bit more than emitters are, and having in mind that the systems needs to read signals coming from one of the emitters in the upper and lower receivers, then, and depending on distance to receivers, the final recommended inclination angle of portable rod is about 10 degrees. This not too important limitation could be circumvented using spherically omnidirectional transducers valid for air transmission (not yet available on the market).

The electronic circuitry designed to excite these PVDF transducers using batteries of 12 volts (NiMH) is depicted in figure 5. Using a linear regulator (7808), this circuit permit powering voltages between 15 and 8.8 volts without any change in the amplitude of the emitted signal. This factor is important to make that emitted signals are consistent independently of the charge state of batteries. And additional circuity is used to detect when batteries are below 9 volts and need to be recharged. The transformer which had to be designed especially for this application has an amplification gain of 20 (5 turns on the first coil and 200 on the second coil using a copper wire of 0.2 mm). Considering the capacitive behavior of PVDF film, the inductance of secondary circuit at the transformer has to be about 75 mH in order to match electronic resonance between coil and PVDF to improve electronic efficiency and acoustical generation. A condenser of 1 mF is connected to the primary coil to provide enough current during transistor's commutation.

The eight receivers used in this prototype are classical Murata piezoelectric ceramic transducers, with a resonant frequency of 40 kHz and good sensitivity, above -65 dB. The reception lobe is conical with an aperture of $\pm$ 80 degrees. Considering this reception lobe, the signal coverage inside the defined working area of 4×4 meters is more than 95%; starting to have some coverage problems (occurring when signals are not received with enough strength at four receivers) just at the borders of the square defining the excavation area. Anyway, whenever the other four receivers which are the farther away from the mobile rod are visible, the trilateration equations can be solved and therefore position can be estimated.

2.4 Software

The software running on the host PC has been designed using Microsoft Foundation Classes (MFC) libraries in order to create a friendly graphical user interface (GUI). The programming language used to code all algorithms was Visual C++. These algorithms perform in a centralized way most of the operations of this sensor system except handshaking and synchronization via radio, that is, sampling the acquisition channels, measuring times of flight (TOF) for each of the eight individual channel, and the trilateration position estimation for each emitter on the portable rod. Additionally the software provides a large number of configuration panels and graphical representations of received signals, TOF estimations, position of emitters XYZ, and rod pose; all these information in real-time. The 3D graphical representations was done using National Instruments CVI Active-X controls.This versatile software allowed as to refine our algorithms by means of visualizing the dataflow before and after each processing function. The measured contour was tested to be accurate enough, as we will see later, using this graphical interface.

3 Position estimation method

The positioning estimation process consists of two steps: (a) computation of the times of flight (TOFs) of each ultrasonic wave travelling from emitters to receivers, and (b) use of the ranging data (obtained multiplying times of flight by speed of sound) to compute the object position by multi-lateration techniques. They are discussed in the two following subsections.

3.1 Time of flight computation

In order to estimate the TOF several algorithms have been tested [17]. Two main types of algorithms were tested offering good performance, reliability and simplicity. One method is based on the slope of the signal envelope, and the other relies on carrier signal correlation. The first method deals with fitting a straight line on the initial rising zone of the envelope of the received signal. Then the TOF is obtained as the point where the fitting line crosses the time axis. As this estimation method is biased, an offset correction is applied. This method has an associated error due to envelope changes caused by noise, echoes composition and relative angular positioning between emitter and receiver. The uncertainly is usually less than one period (25 μs) which implies distance errors of less than 8 mm, and in practice, standard deviations lower than 1.5 mm in laboratory and still air conditions.

The carrier signal correlation method for TOF calculation uses a reference signal captured from a typical reception. The incoming and the reference signal used for correlation are typical narrow-banded signals containing several cycles having a period of 25 μs (period of a 40 kHz signal) modulated in amplitude by a smooth envelope. The more similar the reference and the incoming signal are, the higher the peak value the correlation function returns. Although the results are more accurate than those obtained by the envelope method, the correlation algorithm has associated an uncertainty known as the ambiguity problem. The correlation output is also periodic (see fig. 6 left) with the same frequency as the ultrasonic signals, i.e. in our case, has maxima every 25 μs. In the case of our narrow-band resonant transducers, the relative peak levels are very close and noise can cause that the measured maximum of the correlation corresponds to a neighboring peak of the true maximum, which would amount to an error of one (or more) periods. When bandwidth is limited and signal-to-noise ratio (SNR) is below a certain threshold, the results of TOF standard deviation can move from the Cramer-Rao bound region (low uncertainty) to the Baranking bound region (high uncertainty) (see fig. 6 right) [18]. It implies that TOF estimations can be influenced by errors of an integer number of periods, typically ± 25 μs or ± 50 μs.

Finally, we used the carrier signal correlation method because is more accurate providing estimations with a low standard deviation, and because is not biased when the correct reference signals are selected. The problem of uncertainty is managed using some heuristics and filtering techniques, which avoid that wrong TOFs affect the final 3D position estimation, as we will present in next subsection.

3.2 Position estimation by multi-lateration

If for each receiver k at known position (x_k, y_k, z_k) it is measured the TOF, t_k, it takes the signal to travel from an emitter of unknown position (x, y, z), then multiplying them by the speed of sound, v_s, we obtain a set of ranges r_k from the emitter to each individual receiver k. Writing down the equation of a sphere of radius r_k centered at each receiver position (x_k, y_k, z_k) (eq. 1), we obtain a system of N equations, whose solution tell us the position (x, y, z) of emitter on-board portable rod.

$$\sqrt{(x_k - x)^2 + (y_k - y)^2 + (z_k - z)^2} = v_s \cdot t_k = r_k \tag{1}$$

where, v_s is the speed of sound in air, t_k the time of flight (TOF) of the ultrasonic signal travelling from the emitter to the receiver k.

This method of finding the unknown position (x, y, z) from a set of ranges r_k is called trilateration when $N = 3$, and multi-lateration if $N > 3$. In fact is based on the intersection of spheres, the point where all spheres intersect is precisely the solution in search (x, y, z).

The method that we implemented made use of a redundant configuration of receivers to achieve a more accurate and robust estimation. Redundant means that more receivers than the strictly needed are used, that is to say, the system of equations has more equations than unknown variables (overdetermined). Therefore, the solution is found in a least square sense using the trilateration equation (1) for each receiver with valid TOF measurement.

This LS method is based on an iterative process (Marquant-Levenberg [19]) that minimizes the sum of errors squared. The traditional pseudo-inverse method based on the linearisation of equation (1), then expressing it in matrix form, and next inverting a matrix, was not used to avoid situations where singularities appear (matrix determinant equals zero). These singularities are caused, for example, when all receivers with valid TOFs, are at the same plane. In that case two solutions exists at both sides of the plane, and so, there is no way for this algorithm to incorporate additional information in order to choose the right solution. That problem do not affect the Marquant-Levenberg algorithm since we can give him a-priori information, for example in form of a close-to-solution initial seed, to guarantee that the process converges to the right solution.

If we consider the speed of sound, v_s , also as an unknown, this parameter can be estimated with more precision than using a temperature sensor, so the position estimation is more accurate. At least five valid measurements are needed if position and speed of sound, (x, y, z, v_s), are to be calculated. Then, using our redundant configuration of eight receivers, the estimation can be done even in the case that three receivers do not capture valid TOF measurements.

Finally, the multi-lateration algorithm returns the co-ordinates of both emitters in the portable rod. By extrapolation the position of the lower extreme of the rod is computed. However the LS estimation method used is valid for gaussian noise in the measured TOFs. If one of the TOF are by far wrong (outlier), them the final estimation is degraded strongly. Some heuristics (check of consistency) are used to eliminate false or incongruent estimations. For example, the estimated distance between both emitters in a rod must be very close to its known value (70 cm). Order and median filtering algorithms are used to cope with outliers noise [10]. Some outliers (non-gaussian noise) come from the problem (described in last subsection) of ambiguity in the determination of TOFs in steps of one period, and from specular or multi-path effects. Once the outlier noise is filtered out, the remaining normal distributed fluctuations

are smoothed by averaging.

4 Position estimation in windy conditions

4.1 Wind influence on position estimation

The speed of air influences strongly the speed for ultrasound to propagate in air. Therefore, the apparent speed of sound when a sound propagates between an emitter and a receiver is different when air is still or in motion. If we decompose the speed of air in two components (see fig. 7): 1) v_{al}, that we call *longitudinal speed of air* or the speed of air projected onto the straight line joining emitter to receiver; and 2) v_{at}, called *transversal speed of air* or air orthogonal to the emitter-receiver line; then the apparent speed of sound, v_{sa}, which can be higher or lower to the speed of sound in still air, v_s, is [20]:

$$v_{sa} = v_{al} + v_s\sqrt{1 - (v_{at}/v_s)^2} \tag{2}$$

The above expression (eq. 2) can be approximated in some cases where the speed of air, v_a, is not too high when compared to the speed of sound v_s (for example $v_a < 10$ m/s or equivalently $v_a < 36$ km/s), neglecting the transversal component by this expression:

$$v_{sa} \simeq v_{al} + v_s \tag{3}$$

The influence of air on estimations is important. When using the trilateration equation (eq. 1) that assumes that v_s is known and that there is no airflow, then the estimated position fixes $\{x, y, z\}$ are biased by a distance δr (eq. 4) proportional to the actual wind speed v_{al} along the emitter-receiver$_k$ axis:

$$\delta r = r_k(v_{al}/v_s) \tag{4}$$

In a practical case, for ranges around 3-4 m, a magnitude of 1 m/s in the wind speed causes an error about 1 cm. This is the reason why a moderate wind (above 0.5 m/s) causes errors greater than our specifications (5 mm positioning accuracy), so the challenge in this research was the attenuation of these disturbing wind effects.

4.2 Wind compensation method

The more intuitive method for wind compensation can be based on the extension of equation 1 to the following complex trilateration equations (eq. 5 and 7) that contain as unknowns the components of air speed $\{v_{ax}, v_{ay}, v_{az}\}$.

$$t_k = \frac{r_k}{v_s + v_{al}} \tag{5}$$

where r_k is the unknown real distance between emitter and receiver$_k$, i.e. $\sqrt{(x_k - x)^2 + (y_k - y)^2 + (z_k - z)^2}$, and v_{al} is a function of its cartesian components in this manner

$$v_{al} = \vec{v}_a \cdot \vec{u}_k = \frac{v_{ax}\,(x_k - x) + v_{ay}\,(y_k - y) + v_{az}\,(z_k - z)}{r_k} \tag{6}$$

being, $\vec{u}_k$ the unitary vector oriented along the line connecting the emitter with receiver k.

Substituting equation (6) into equation (5), then the final multi-lateration equation to be used is:

$$t_k = \frac{r_k^2}{v_s r_k - v_{ax}(x - x_k) - v_{ay}(y - y_k) - v_{az}(z - z_k)} \tag{7}$$

The air compensation method based on equation (7) would need a minimum of 7 TOA's measures to be made in order to deduce the unknowns: $\{x, y, z, v_s, v_{ax}, v_{ay}, v_{az}\}$. In principle, this method is feasible and works well in simulations using homogeneous wind and ideal TOA values without noise, but it does not provide good results when the TOA values have a certain quantity of any kind of noise (for example gaussian noise with 2 microseconds of standard deviation as is common in any real implementation).

After some analysis about the cost function to be minimized and its singularities, we concluded that there was no way to estimate simultaneously localization and air speed using equations eq. 7. On the contrary, we learnt that it is possible to estimate speed of sound and speed of wind simultaneously with high precision using a reference consisting of an emitter placed at a known position. Therefore, the final compensation of wind effects was done in two stages using in both cases equation (7):

- 1) Estimate speed of air v_a and speed of sound v_s using a reference station at a known location x_b, y_b, z_b
- 2) Estimate x, y, z using the now known values of v_a and v_s)

This compensation method should work perfectly, whereas the wind flow along the working volume were uniform; in cases of turbulence we predict that the compensation could be moderate or even poor.

5 Experimental results

The position measurement system has been tested indoors and outdoors, i.e. in an environment free of wind and with typical airflows (below 5 m/s), respectively. Figure 8 shows some indoors-experimental data returned by the 3D ultrasonic sensor. Measurements shown at the left side of figure 8 is a plot of X-Y estimations by placing the portable rod on a fixed point and taking continuous measurements during some minutes. The middle plot in this figure display the X-Z estimation for the same case. Right plot in figure 8 was obtained moving the rod following a trajectory drawn on a paper, consisting of a increasing burst-pulse (from 1 mm to 1 cm). This last type of tests were performed to evaluate the system resolution and its capability to make sketches.

The test results have been summarised in Table 1. The *single emitter* column summarises the performance obtained in the position estimation of one of the two emitters on the portable rod. The *base of rod* column indicates the performance in estimating the position at the tip of the rod by extrapolation of single estimations for the two emitters on the portable rod. It can be seen that there is an error amplification factor about 2.5, which is due to the so-called "lever effect", that is to say, due to the separation of both emitters on the rod (70 cm) with regard to the total rod length (200 cm) which produces an amplified propagation of errors from emitters positions to the rod's tip.

In this table (tb. 1), *accuracy* deals with the difference between the position given by the system and the real position; i.e. this parameter is equivalent to the absolute error. The *repeatability* of the measurement is related to the radius of the circumference that circumscribes 3σ of the measurements made by the system at a fixed position. The *resolution* term is used in these tests to indicate the minimum contour dimension for which the system can draw a recognisable pulse-like contour.

Airflow errors are significantly reduced by the strategy of using an additional differential emitter. Figure 9 shows an example of how the airflow compensation method works. One thousand location estimations were recorded during ten minutes for emitter number 2 positioned at location x=85 mm, y=-60 mm and z=1200 mm. In this case, the differential emitter was placed approximately 1 meter apart from the transducer used in these tests (emitter number 2). The maximum wind speed measured with an anemometer was 5

m/s. There was a maximum error, due to airflows, of 50 mm without compensation, but after differential compensation the localisation error diminished to no more than 10 mm. This compensation method achieve significant improvements, the main benefits are: (a) offset or systematic error elimination (b) less standard deviation. As expected, the quality of compensation depends on the distance from the rod to the differential emitter. The larger this separation, the less performance in wind-influence compensation. This fact is especially true for turbulent airflows, meanwhile wind effects due to uniform and laminar airflows are better compensated. All these tests were carried out outdoors in a near-by land outside our laboratory simulating an archaeological site of 16 m^2. Other tests were made at the "Gran Dolina" archaeological site in Atapuerca, Burgos (Spain).

6 Conclusions and future development

In this paper it has been presented a new ultrasonic position measuring system for location of found objects in archaeological findings. This system can increase the efficiency and cancel out human errors during the localisation of findings, contour tracing and database transfer processes. The system, once it is configured and calibrated, is very easy to use for an archeologist. There are mainly two possible ways of operation: 3D position measurement and contour drawing. This prototype has been verified in laboratory conditions, outside our laboratory, and in the *Atapuerca* paleo-archaeological excavation site. Precisions obtained with the ultrasonic device were below 10 mm in indoors or still air conditions. Wind influences strongly position measurements, but the described differential correction method attenuates errors considerably allowing the operation outside with winds up to 5 m/s. Contour tracing tests were made with real objects, obtaining well defined and accurate contours for objects of interest, which are those greater than 10 mm.

There are some future plans to improve even more the performance of the system presented in this paper, especially regarding scalability and wind effect cancellation. The computation of TOF's and location of each rod is centralized on a PC platform, therefore it could be a bottle neck when expanding the system to cover wider working areas. As the number of receivers increases, the system needs more time to make all the calculations and, therefore, the number of measurements per second is decreased. In order to avoid this effect, a new kind of receiver module is being designed. The new receiver will have its own signal conditioning circuit and a dedicated signal processor (DSP) which will give the system a parallel processing architecture and an easier way for the system to be extended by adding more rods and receivers. On the other hand, a new method of compensation based on bi-directional transmission of ultrasound is being considered. The idea is to cancel out the influence of

the longitudinal air component v_{al}. This method would allow the system to operate outdoors with similar precisions to that which were obtained indoors, independently of the airflows in the workspace.

References

[1] Cervera, Arsuaga, and Bermudez et al, Atapuerca: Un millón de años de historia, Plot Ediciones y Editorial Complutense, 1998.

[2] H.R. Everett, Sensors for mobile robots. Theory and applications, A.K. Peters, Ltd. Wellesley, Massachusetts, 1995, p. 528.

[3] J. Hightower and G. Borriello, Location systems for ubiquitous computing, IEEE Computer, 34 8 (2001) 57–66.

[4] R. Want, A. Hopper, V. Falcao, and J. Gibbons, The active badge location system, ACM Transations Information Systems, 10 1 (1992) 91–102.

[5] Arc Second Inc, Constellation-3d- indoor gps technology for metrology, White paper 071502, (2002) 1–11.

[6] J.F. Figueroa and J.S. Lamancusa, A method for accurate detection of time of arrival: analysis and design of an ultrasonic ranging system, Journal Acoustical Society of America, 91 1 (1992) 486–494.

[7] H.W. When and P.R. Belanger, Ultrasound-based robot position estimation, IEEE Transaction on Robotics and Automation, 13 5 (1997) 682–692.

[8] A. Mahajan and F. Figueroa, An automatic self-installation and calibration method for a 3d position sensing system using ultrasonics, Robotics and Autonomous Systems, 28 (1999) 281–294.

[9] J.M. Martin-Abreu et al, Measuring the 3d-position of a walking vehicle using us and em waves, Sensors and Actuators A, 75 2 (1999) 131–138.

[10] J.M. Martín-Abreu, A.R. Jiménez, F. Seco, L. Calderón, J.L. Pons, and R. Ceres, Estimating the 3d-position from time delay data of us-waves: Experimental analysis and new processing algorithm, Sensors and Actuators A, 101 (2002) 311–321.

[11] N.B. Priyantha, A. Chakraborty, and H. Balakrisnan, The cricket location support system, ACM/IEEE Int. Conference On mobile Computing and Networking, Boston, USA, August, 2000, p. 32-43.

[12] Mike Hazas and Andy Ward, A novel broadband ultrasonic location system, Proceedings of UbiComp 2002: Fourth International Conference on Ubiquitous Computing, Goteborg, Sweden, September, 2002, p.264–280.

[13] J. Werb and C. Lanzl, Designing a positioning system for finding things and people indoors, IEEE Spectrum, September (1998) 71–78.

[14] P. Bahl and V.N. Padmanabhan, Radar: An in-building user location and tracking system, Proceedings of the IEEE Infocom, Tel Aviv, Israel, 2000, p.775–784.

[15] D. Niculescu and B. Nath, Ad hoc positioning system (APS) using AOA, In proceedings of the INFOCOM, San Francisco, CA, 2003.

[16] Measurement Specialist Inc, 40kHz Omni-directional ultrasound transmitter, Application specification document, 20-3, http://www.msiusa.com, December, 2001.

[17] Billur Barshan, Fast processing techniques for accurate ultrasonic range measurements, Measurement Science Technology, 11 1 (2000) 45–50.

[18] A.J. Weiss and E. Weinstein, Fundamental limitations in passive time delay estimation. Part 1: Narrow-band systems, IEEE Transactions on Acoustics Speech and Signal Pocessing, 31 2 (1983) 472-486.

[19] W.H. Press, S.A. Teukolsky, and W.T. Vetterling, Numerical Recipes in C, Second Edition, Cambridge University Press, 1995, p. 994.

[20] A.R. Jiménez, F. Morgado, and F. Seco, Ultrasound position estimation sensor for precise localisation of archaelogical findings, Eurosensors XVIII, Rome, Italy, 13-15 September, 2004, p.444-445.

Biography

Antonio R. Jiménez, graduated in Physics, Computer Science branch (Universidad Complutense de Madrid, June 1991). He received the PhD degree also in Physics from the Universidad Complutense de Madrid in October 1998. From 1991 to 1993, he worked in industrial laser applications at CETEMA (Technological Center of Madrid), Spain. Since 1994, he is working as a researcher at the Instituto de Automática Industrial, CSIC, Spain. His current research interests include sensor systems (ultrasound in air, laser range-finding) and signal processing techniques for localization, feature extraction and tracking in sectors such as robotics, vehicle navigation, inspection, personal assistance and machine-tool.

Fernando Seco Granja, was born in Madrid, Spain. He has a degree in Physics from the Universidad Complutense in Madrid (1996), and a PhD degree in Physical Sciences from UNED (2002). His dissertation dealt with the development of a linear position sensor based on the transmision of ultrasonic signals in a waveguide. Since 1997, he has been working at the Instituto de Automatica Industrial, CSIC. His research interests include the electromagnetic generation and propagation of mechanical waves in metals, the use of ultrasonic methods in industrial environments and localization systems for people and autonomous vehicles.

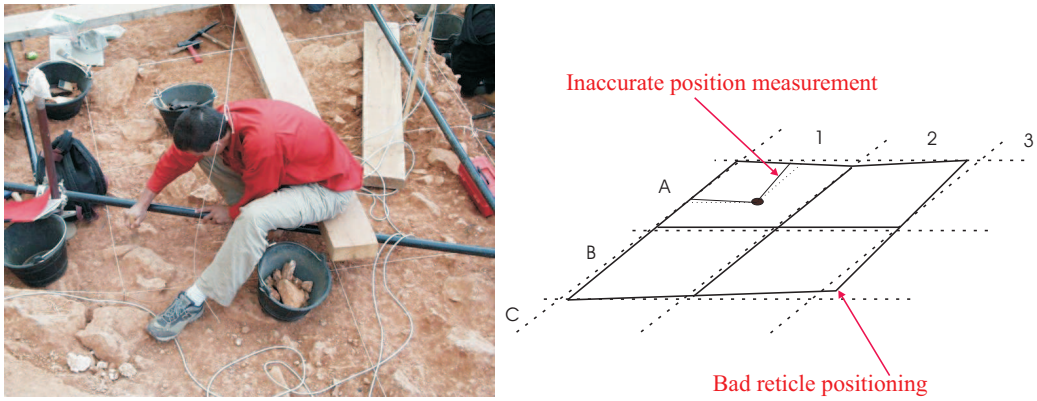

Fig. 1. Positioning errors using a reticle. (left) Detail of a archaeologist working in a 1 meter square cell; (right) sketch of ideal reticle (dot line) and actual set-up with strings (solid line)

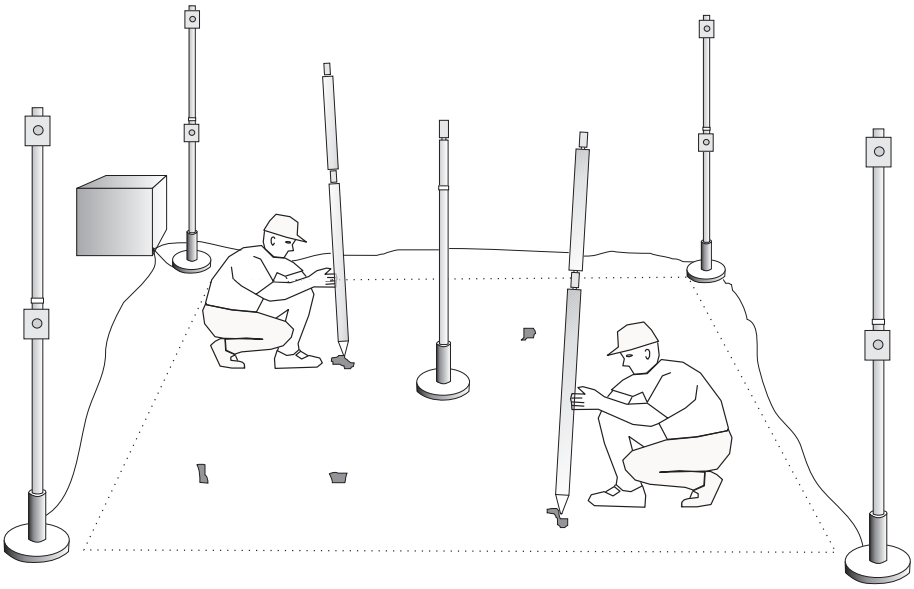

Fig. 2. Using portable rods to localise and draw findings

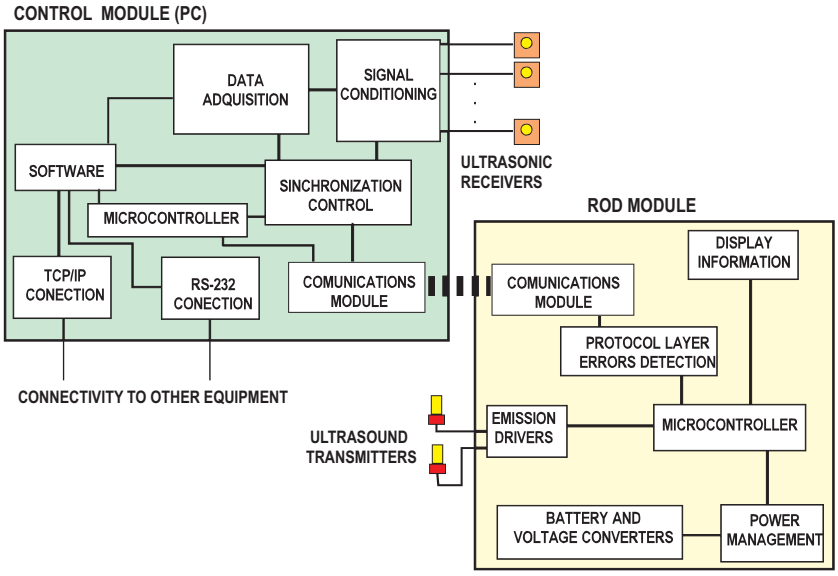

Fig. 3. General block diagram of the localisation system

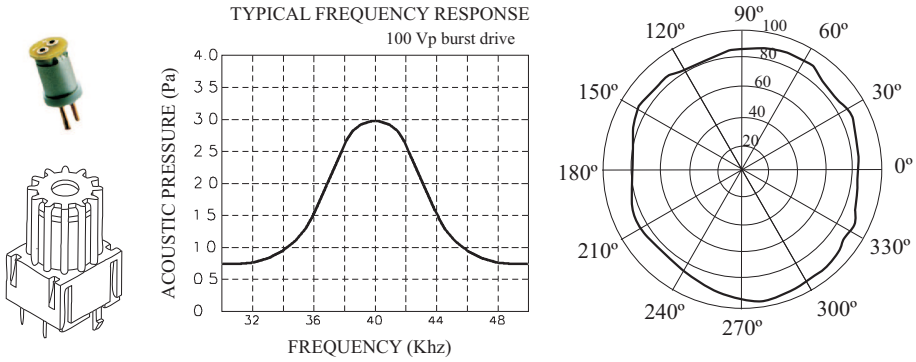

Fig. 4. Omnidirectional PVDF transducer used as emitter. (left) PVDF film is shaped in a cylindrical holding and protected with an external grid; (center) Its frequency response around 40 kHz; (right) horizontal ultrasonic emission lobe

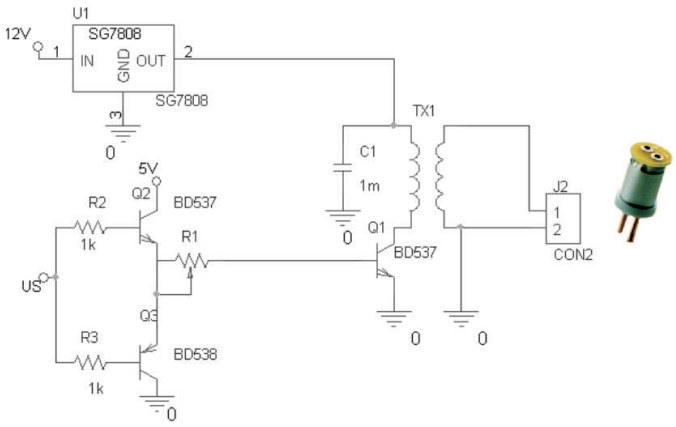

Fig. 5. Electronic circuit for ultrasonic PVDF excitation

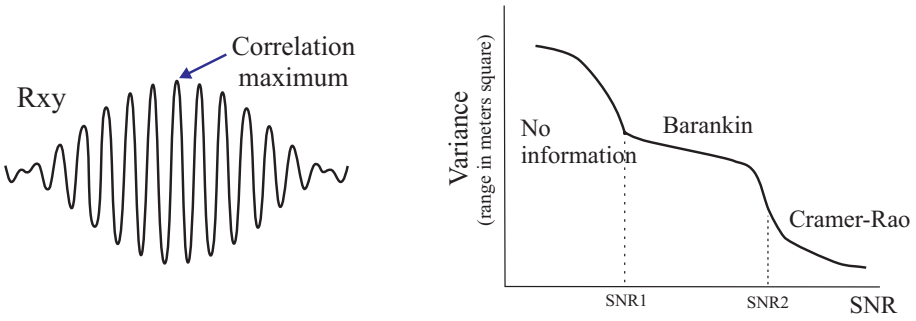

Fig. 6. (left) result of correlating the received signal with the stored reference; (right) Regions where estimation variance changes with SNR at certain thresholds. This thresholds change with bandwidth, duration and frequency of signals

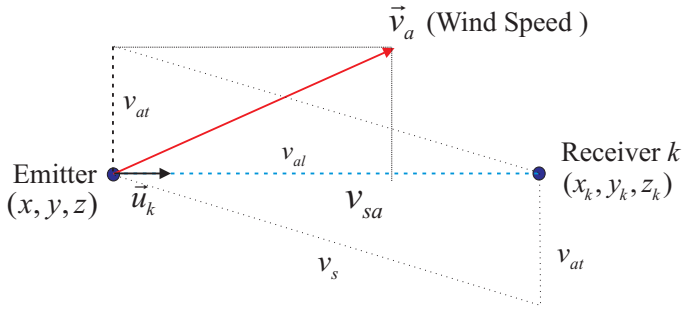

Fig. 7. Air flow components $\vec{v}_a = \{v_{al}, v_{at}\}$ with respect to the emission-reception axis

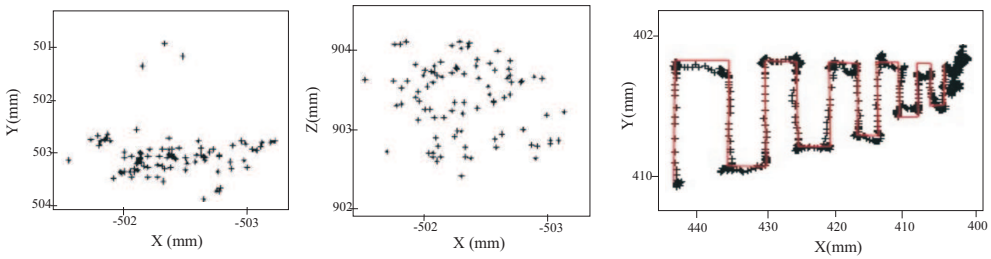

Fig. 8. (left-middle) Accuracy and repeatability indoors tests showing the dispersion in 3D position estimation; (right) Resolution indoors tests performed following a predefined increasing-size pulse-like path

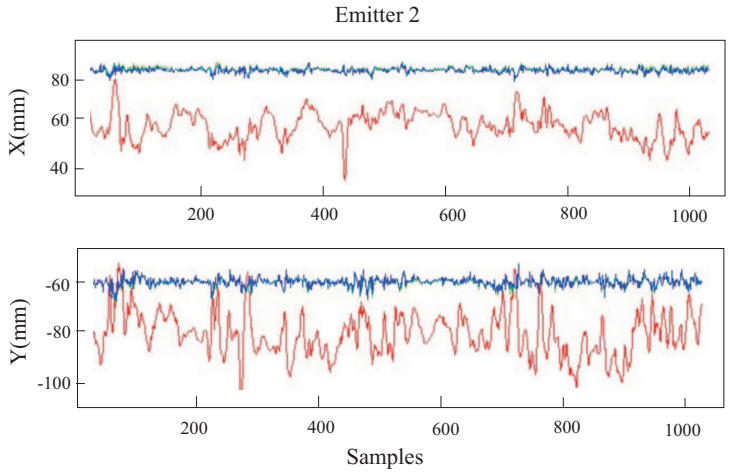

Fig. 9. (light-grey high-variance plots) X and Y estimations under a wind-flow varying between calm condition to 5 m/s speed, which suffer from errors up to 5 cm; (dark-grey low-variance plots) Same case but using the compensation method, a moderate to good compensation (1 cm error still remains) is obtained for this case where reference station is approximately 1 m apart from the real transducer position (x=85 mm, y=-60 mm)

List of Figures

	Single emitter	Base of Rod
Accuracy (mm)	4	10
Repeatability (mm)	3	8
Resolution (mm)	3	6

Table 1
Indoor performance of the 3D ultrasonic sensor

List of Tables